AIP | Applied Physics Letters

Detection of a vortex nucleation position in a circular ferromagnet using asymmetrically configured electrodes

Xiaomin Cui, Shaojie Hu, and Takashi Kimura

Citation: Applied Physics Letters **105**, 082403 (2014); doi: 10.1063/1.4894216
View online: http://dx.doi.org/10.1063/1.4894216
View Table of Contents: http://scitation.aip.org/content/aip/journal/apl/105/8?ver=pdfcov
Published by the AIP Publishing

Detection of a vortex nucleation position in a circular ferromagnet using asymmetrically configured electrodes

Xiaomin Cui,[1] Shaojie Hu,[1] and Takashi Kimura[2,3,4,a)]
[1]*Graduate School of Information Science and Electrical Engineering, Kyushu University, 744 Motooka, Fukuoka 819-0395, Japan*
[2]*Department of Physics, Kyushu University, 6-10-1 Hakozaki, Fukuoka 812-8581, Japan*
[3]*CREST, Japan Science and Technology Agency, Sanbancho, Tokyo 102-0075, Japan*
[4]*Research Center for Quantum Nano Spin Sciences, 6-10-1 Hakozaki, Fukuoka 812-8581, Japan*

(Received 8 July 2014; accepted 17 August 2014; published online 26 August 2014)

We demonstrated that the anisotropic magneto-resistance of a ferromagnetic micro-disk measured by the asymmetrically configured electrodes provide the information of the vortex chirality. The large difference of the electrical resistivity between the ferromagnetic disk and the nonmagnetic electrodes creates an inhomogeneous current distribution, allowing us to detect the local domain structure. By focusing on the chirality-dependent magneto-resistance change due to the vortex nucleation, we can clearly detect the vortex nucleation position, leading to the chirality determination. The reliability of the developed detection method has been confirmed by the magneto-resistance measurement with symmetrically configured electrodes. © *2014 AIP Publishing LLC*.
[http://dx.doi.org/10.1063/1.4894216]

Study on magnetic vortex structure stabilized in a micron or submicron scaled ferromagnetic disk has been paid of great attention because of its high thermal stability, negligible magneto-static interaction, and low frequency dispersion at the resonant state.[1–6] These outstanding characteristics provide prospective application in high density storage media[7] and functional radio-frequency (RF) devices such as reconfigurable RF filter[8–10] and spin torque oscillator.[5] Moreover, the magnetic vortex includes several intriguing fundamental properties such as Bloch point reversal[11] and the critical slowing down of the vortex formation.[12] The vortex structure can be characterized by two important quantity: polarity[2,4] (the direction of the vortex core, either up or down), and chirality (rotational direction of the magnetization, clockwise (CW) or counterclockwise (CCW)).[13] The effective manipulation and identification of the vortex characteristics are indispensable for the realization of aforementioned applications and further understanding the fundamental property of the magnetic vortex.

So far, numerous reports concerning the manipulation of the vortex polarity and chirality have been developed.[14,15] In addition, the detection methods for the polarity and chirality have also been developed by several specific measurement techniques such as Magnetic Force Microscope (MFM),[2,16,17] Lorentz microscope,[18,19] or Magneto-optical Kerr effect (MOKE).[20] However, in these techniques, complex experimental conditions such as measurement time, temperatures, and sample thickness have to be satisfied. These regulations prevent the systematic and statistical considerations. The lateral spin valve also can detect the vortex chirality.[21,22] However, the complicate fabrication process and a tiny spin-dependent signal may prevent the fair evaluation of the vortex structure at room temperature. In the method using anisotropic magnetoresistance (AMR) with four terminal electrodes, the device can be fabricated more simply.[23] However, the analysis based on the micromagnetic simulation may prevent the intuitive understanding. Therefore, to further explore the new functionalities of spin vortex and deepen the understanding on fundamental property of the vortex structure, we should seek a relatively simple and reliable method to identify the vortex chirality.

To detect the vortex chirality, in the present study, we use an AMR effect, in which the resistance of the ferromagnet depends on the magnetic domain structure. In the ferromagnetic disk, the magnetization reversal proceeds through the nucleation, displacement, and annihilation of the vortex.[3] The nucleation position is known to depend on the direction of the applied magnetic field and the vortex chirality. Since the nucleation of the vortex core corresponds to the phase transition of the domain structure from the uniform magnetization state,[12] a significant AMR change is induced by the nucleation of the vortex, especially around the vortex core. As schematically shown in Figs. 1(b) and 1(c), the domain structure before the nucleation can be described by a similar curling structure with setting the vortex core outside the disk. Since the spin distribution inside the disk seems a C shape, this domain structure is known as C state.[24] Here, we introduce asymmetrically configured nonmagnetic Cu electrodes, which are schematically shown in Fig. 1(a). Because of the large difference in the resistivity between the ferromagnetic disk and the Cu electrodes, the electric current flows favorably in the Cu electrode, leading to create an inhomogeneous current distribution. This enables to detect the local domain structure around the bottom side of the ferromagnetic disk. Therefore, when the vortex nucleates from the bottom side, we should observe the large resistance change because the most of the spins inside the electrode rotates from the horizontal direction.(Fig. 1(b)) On the contrary, the vortex nucleation from the opposite side will be undetectable in the AMR measurement using the same electrode because the current flowing in the top side is so tiny.(Fig. 1(c)) In this way, we can distinguish the vortex

a)t-kimu@phys.kyushu-u.ac.jp

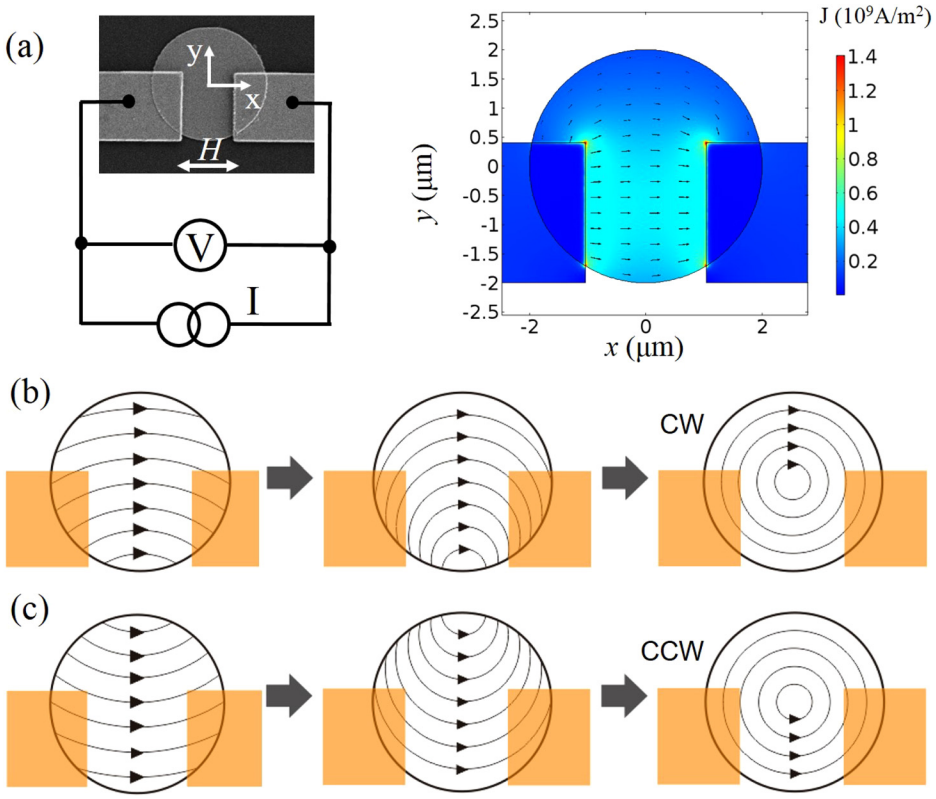

FIG. 1. (a) Scanning electron microscope image of the fabricated device together with a probe configuration for the AMR measurement and numerically obtained 2-dimensional current-density distribution in a ferromagnetic disk with 4 μm diameter. The magnetic field is applied along the horizontal axis, parallel to the average current direction (longitudinal configuration). Schematic illustrations of the vortex nucleation processes for CW chirality (b) and CCW chirality (c). Here, the magnetic field is reduced from the positive saturation field.

chirality by monitoring the resistance of the local area of the ferromagnetic disk.

We have prepared the sample consisting of a Permalloy (Py) disk, a diameter of 4 μm and a thickness of 40 nm and a pair of the nonmagnetic Cu electrodes, 200 nm thickness. Figure 1(a) shows a scanning electron microscope image of the fabricated sample together with the schematic configuration used for the AMR measurement. The Py disk was fabricated by using a conventional lift-off method combined with the electron beam lithography. The Cu electrodes were deposited by a Joule heat evaporator after the surface cleaning of the Py disk by a low energy Ar ion milling. Here, the vertical position of the Cu electrodes is shifted by 800 nm from the center of the disk. The electrical resistivity for the Py is 29 $\mu\Omega$ cm, much larger than that for the Cu electrode (2.2 $\mu\Omega$ cm). The AMR measurement was performed by two-terminal resistance measurement with a low bias ac of 55 μA. Here, the magnetic field is applied along the horizontal direction, meaning the longitudinal configuration.

To confirm that the large difference in the resistivity between the Py and Cu makes an inhomogeneous current distribution in the ferromagnetic disk, we have calculated two dimensional distribution of the current density in the AMR device configured similarly to the fabricated device by using COMSOL multiphysics. As shown in Fig. 1(a), the current in the Py disk is found to flow mainly in the bottom part of the Py disk. This enables to detect the local domain structure of the Py disk.

Figure 2 shows a representative result of the AMR curve measured at room temperature. In both the forward and backward field sweeps, when the magnetic field is reduced from the saturation state, the sudden resistance change is observed at 10 Oe. These sudden changes correspond to the nucleation of the vortex core in the ferromagnetic disk. After the sudden change, the resistance gradually increases with approaching to the value for the saturation state. The inset in Fig. 2 represents the domain structures calculated by OOMMF just after the vortex nucleation. As mentioned above, since the resistance change is dominated by the domain structure in the bottom side of the ferromagnetic disk, the sudden resistance changes observed in Fig. 2 indicate that the vortex nucleates from the bottom edge of the disk both in the forward and backward sweeps. Therefore, the vortex chiralities in the backward and forward sweeps can be

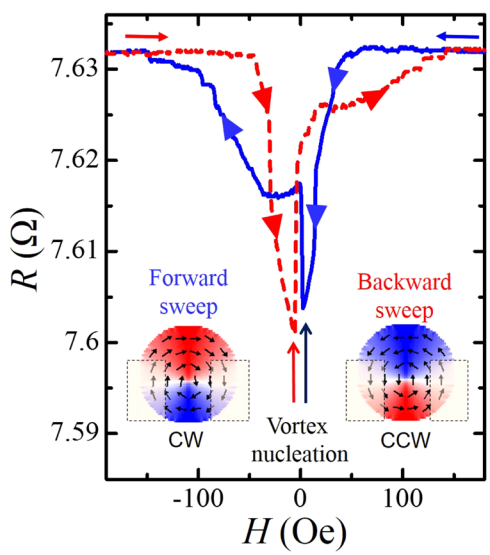

FIG. 2. Longitudinal AMR curve of the circular disk measured at room temperature. Solid and dotted lines correspond to the forward and backward field sweeps, respectively, while the inset shows the numerically calculated magnetization reversal process of the disk for the backward and forward sweeps.

determined as CCW and CW, respectively, as schematically shown in the inset of Fig. 2.

From the aforementioned consideration, when the vortex nucleates from the top side, the nucleation of the vortex may become undetectable. However, as mentioned above, the observed MR curve always involves the sudden change around 10 Oe in the conventional field sweep, indicating the vortex always nucleates from the bottom side. To realize the formation of the reversed vortex, the maximum magnetic field during the field sweep was reduced. This is because the C-state just after the annihilation of the vortex is known to induce the nucleation of the vortex from the annihilated side.[24,25] Figure 3 shows the magnetoresistance curve in the field range $-150\,\text{Oe} < H < 200\,\text{Oe}$. As expected above, in the backward sweep, the MR curve without the sudden resistance change has been observed, which means the vortex nucleates from the top side and the chirality should be CW for both backward and forward sweeps. In addition, it should be noted that the small resistance jump has been observed at 132 Oe. This small jump can be understood by the annihilation of vortex from the bottom side. The experimental fact that the small resistance change due to the vortex annihilation has not been observed in Fig. 2 is also consistent with the local detection of the domain structure. Thus, we can simply distinguish the vortex chirality from the shape of the AMR curve.

By using the simple evaluation method, we extend to evaluate how the vortex chirality distributes with changing the magnitude of the reversed magnetic field H_r. Figure 4 shows the probability of the formation of CW and CCW chiralities as a function of H_r. Here, the probability at each point was calculated by repeating the AMR measurement for 10 times. It can be clearly seen that the probability of CCW chirality formation increases with increasing H_r and reaches 100% at $|H_r| > 160\,\text{Oe}$. The probability is 50% at $|H_r| \approx 135\,\text{Oe}$, indicating that two possible chiralities CW and CCW were randomly formed. Since in an ideal

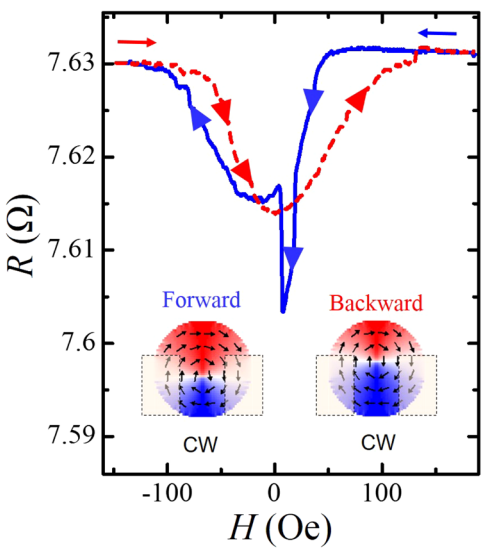

FIG. 3. Longitudinal AMR curve in the field range from 190 Oe to −150 Oe. The magnetic field is swept from 190 Oe to −150 Oe and then swept back to 190 Oe. Solid and dotted lines correspond to the forward and backward field sweeps, respectively, with the inset of numerically calculated magnetization reversal process of the disk for the backward and forward sweeps.

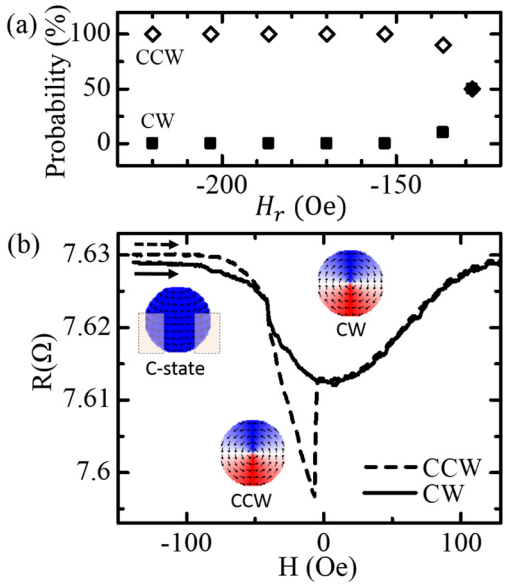

FIG. 4. (a) Probability of the CW (solid square) and CCW (open square) vortex formation as a function of the reversed magnetic field. (b) Representative AMR curve for chirality of CW (solid line) and CCW (dotted line) during sweep from −150 Oe to 190 Oe and the C-state domain structure after the annihilation field.

ferromagnetic disk, the chirality should be randomized because of its symmetric shape, this result indicates that the energy barrier for the formation of the vortex from the bottom side is reduced. To explain this, we consider the influence of slight geometrical asymmetry due to the surface cleaning. As explained above, the surface of the Py electrode underneath the Cu electrode was cleaned by Ar ion milling. This geometrical modification reduces the formation energy of the vortex from the bottom side although the etched depth is less than 2 nm, about 5% of the total thickness. The reasons for the field dependence of the probability may be due to a residual domain structure, namely, C-shaped domain structure shown in the inset of Fig. 4(b), just after the annihilation. The domain structure of the ferromagnetic disk is known to remain the curling feature when the external magnetic field is not sufficiently large for the saturation of the magnetization, similarly to the situation just before nucleation. This remaining domain structure tends to form the vortex from the top side. Thus, 50% probability around the annihilation field can be understood by the competition between the non-saturated and the geometrical asymmetric effects.

To obtain further evidence for the advantage of Py disk with asymmetrically configured electrodes, we also fabricated another AMR device consisting of a Py disk with the Cu electrodes located in the central position. Here, the dimension of the ferromagnetic disk is exactly same as that in the previous experiment. Since the Cu electrodes are located in the center of the disk, the vortex formation from both the top and bottom sides can be observed as a sudden resistance change with the same magnitude. Therefore, the chirality cannot be distinguished from the AMR measurement. To confirm this scenario, we evaluate the AMR curve under the field sweep from −135 Oe to 190 Oe. Since the annihilation field is −130 Oe, we expect that the domain structure is not fully saturated at −135 Oe. Figure 5 shows a

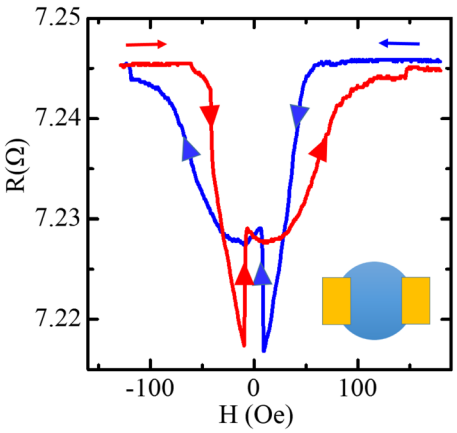

FIG. 5. Longitudinal AMR curve of the Py circular disk measured by the symmetrically configured electrode. Since the reversed magnetic field is close to the annihilation field, the position of the vortex nucleation may be reversed in each sweep.

representative longitudinal AMR curve under the field sweep. The observed AMR curve for each sweep is almost symmetric with respect to the field sweep direction. Importantly, the large resistance jump at 10 Oe due to the vortex nucleation is clearly observed in both sweep. As mentioned above, the C-state domain structure tends to maintain the chirality in the reversed field sweep, the vortex nucleation side in the forward and backward sweep should be opposite each other. However, the observed AMR curve shows the same feature during 10-time repetition of the measurements. This is consistent with the above expectation that the vortex nucleation from the top and bottom sides provides the same contribution in the AMR. Thus, we cannot distinguish the vortex chirality from the AMR curve measured by the symmetrically configured electrode.

In short, we have studied the AMR curve for a single Py circular disk measured by nonmagnetic Cu electrodes with the resistivity much lower than that for the Py disk. We showed that the asymmetrically configured electrode makes it possible to distinguish the vortex chirality in the relatively simple way. By extending this simple detection method, the vortex chirality in the AMR device is found to depend on the magnitude of the maximum magnetic field. The importance of the asymmetric configuration of the electrode is examined by evaluating the AMR device with the symmetrically configured electrodes. This simple and reliable method for the chirality detection may accelerate the development on the characterization of magnetic vortex and its future spintronic application.

This work was partially supported by KAKENHI (26630162), CANON Foundation and CREST. The authors (X.C. and S.H.) acknowledge the China Scholarship Council for Young Scientists.

[1]R. P. Cowburn, D. K. Koltsov, A. O. Adeyeye, and M. E. Welland, Phys. Rev. Lett. **83**, 1042 (1999).
[2]T. Shinjo, T. Okuno, R. Hassdorf, K. Shigeto, and T. Ono, Science **289**, 930 (2000).
[3]K. Yu Guslienko, V. Novosad, Y. Otani, H. Shima, and K. Fukumachi, Phys. Rev. B **65**, 024414 (2001).
[4]R. Antos, Y. Otani, and J. Shibata, J. Phys. Soc. Jpn. **77**(3) 031004 (2008).
[5]V. S. Pribiag, I. N. Krivorotov, G. D. Fuchs, P. M. Braganca, O. Ozatay, J. C. Sankey, D. C. Ralph, and R. A. Buhrman, Nat. Phys. **3**, 498–503 (2007).
[6]V. Novosad, M. Grimsditch, J. Darrouzet, J. Pearson, S. D. Bader, V. Metlushko, K. Guslienko, Y. Otani, H. Shima, and K. Fukamichi, Appl. Phys. Lett. **82**, 3716–3718 (2003).
[7]N. Nishimura, T. Hirai, S. Koganei, T. Ikeda, K. Okano, Y. Sekiguchi, and Y. Osada, J. Appl. Phys. **91**, 5246 (2002).
[8]V. Novosad, F. Y. Fradin, P. E. Roy, K. S. Buchanan, K. Y. Guslienko, and S. D. Bader, Phys. Rev. B **72**, 024455 (2005).
[9]J. Shibata, K. Shigeto, and Y. Otani, Phys. Rev. B **67**, 224404 (2003).
[10]J. Shibata and Y. Otani, Phys. Rev. B **70**, 012404 (2004).
[11]A. Thiaville, J. M. Garcia, R. Dittrich, J. Miltat, and T. Schrefl, Phys. Rev. B **67**, 094410 (2003).
[12]S. Savel'ev and F. Nori, Phys. Rev. B **70**, 214415 (2004).
[13]M. Grimsditch, P. Vavassori, V. Novosad, V. Metlushko, H. Shima, Y. Otani, and K. Fukumichi, Phys. Rev. B **65**, 172419 (2002).
[14]B. van Waeyenberge, A. Puzic, H. Stoll, K. W. Chou, T. Tyliszczak, R. Hertel, C. H. Back, and G. Schutz, Nature **444**, 461–464 (2006).
[15]K. Yamada, S. Kasai, Y. Nakatani, K. Kobayashi, H. Kohno, A. Thiaville, and T. Ono, Nat. Mater. **6**, 270–273 (2007).
[16]S. Yakata, M. Miyata, S. Nonoguchi, H. Wada, and T. Kimura, Appl. Phys. Lett. **97**, 222503 (2010).
[17]M. Jaafar, R. Yanes, F. Perez de Lara, O. Chubykalo-Frsenko, A. Asenjo, E. M. Gonzalez, J. V. Anguita, M. Vazquez, and J. L. Vicent, Phys. Rev. B **81**, 054439 (2010).
[18]M. Schneider, H. Hoffmann, and J. Zweck, Appl. Phys. Lett. **79**, 3113 (2001).
[19]M. Schneider, H. Hoffmann, and J. Zweck, Appl. Phys. Lett. **77**, 2909 (2000).
[20]M. Natali, A. Popa, U. Ebels, Y. Chen, S. Li, and M. E. Welland, J. Appl. Phys. **96**, 4334 (2004).
[21]T. Kimura, Y. Otani, and J. Hamrle, Appl. Phys. Lett. **87**, 172506 (2005).
[22]S. Yakata, M. Miyata, S. Honda, H. Itoh, H. Wada, and T. Kimura, Appl. Phys. Lett. **99**, 242507 (2011).
[23]P. Vavassori, M. Grimsditch, V. Metlushkko, and B. Ilic, Appl. Phys. Lett. **86**, 072507 (2005).
[24]T. Pokhil, D. Song, and J. Nowak, J. Appl. Phys. **87**, 6319 (2000).
[25]T. Kimura, Y. Otani, H. Masaki, T. Ishida, R. Antos, and J. Shibata, Appl. Phys. Lett. **90**, 132501 (2007).